

THz applications of 2D materials: Graphene and beyond

Minjie Wang*, Eui-Hyeok Yang

Mechanical Engineering Department, Stevens Institute of Technology, Castle Point on the Hudson, Hoboken, NJ 07030, USA

ARTICLE INFO

Article history:

Received 29 July 2017

Received in revised form 22 August 2017

Accepted 22 August 2017

Available online xxxx

Keywords:

Terahertz

Graphene

2D materials

TMDs

ABSTRACT

Monolayer graphene, successfully isolated in 2004, is the first member of the class of materials called two-dimensional (2D) materials. Since then, 2D materials such as hexagonal boron nitride (h-BN), transition metal dichalcogenides (TMDs), silicene and phosphorene have been extensively investigated owing to their extraordinary mechanical, chemical, and physical properties. Furthermore, some of these 2D materials are expected to result in novel high-frequency and optical phenomena. In this review, we highlight the recent progress of the state-of-the-art research on graphene applications on the scale of terahertz (THz) emitting, detecting and modulating, and summarize similar THz applications of h-BN, TMDs, silicene and phosphorene.

© 2017 Elsevier B.V. All rights reserved.

Contents

1. Introduction.....	1
2. Graphene for THz applications.....	2
2.1. Graphene based THz-emitter	2
2.2. Graphene base THz-detector	3
2.3. Graphene THz modulator	3
2.4. Enhancing THz-wave absorption	4
3. Other 2D materials for THz applications.....	4
4. Conclusions and future prospects.....	5
References	6

1. Introduction

The terahertz (THz) frequency range contains frequencies from 0.1 THz to 20 THz (or, equivalently, from 3 cm^{-1} to 600 cm^{-1} , from 0.41 meV to 82 meV, or from 3 mm to 0.02 mm). This frequency range is in between two well-defined frequency regimes – the photonic regime on the higher-frequency (or shorter-wavelength) side and the electronic regime on the lower-frequency (or longer-wavelength) side. This special location implies that one can use optical, electronic, or both optical and electronic means, to generate, detect, or manipulate electromagnetic waves. The THz frequency range is scientifically rich, containing a host of low-energy elementary and collective excitations in condensed matter (i.e., phonons, plasmons, magnons, spin resonances, and superconducting gap excitation) [1–7]. Dynamical phenomena in solids such as carrier scattering [8], recombination [9,10], and tunneling [11–13] typically occur on a time scale of picoseconds, which corresponds to

frequencies in the THz range. The characteristic energy of 4 meV (i.e., 1 THz) corresponds to a temperature of 46 K, which means that one needs to do the measurements at liquid helium temperatures, in order to explore THz phenomena in condensed matter. However, technologically speaking, THz frequency range is poorly developed. No mature solid-state technology exists for the generation, detection, and manipulation of THz electromagnetic waves. Hence, this frequency range is usually referred to as “the last frontier in the electromagnetic spectrum to be exploited” or the “THz technology gap”. However, some recent notable breakthroughs exist, such as 3D numerical simulations of THz generation by two-color laser filaments [14], nonlinear generation of THz plasmons in graphene and topological insulators [15], 28.3 THz nano-rectenna with a rectifier (rectenna) for harvesting infrared energy [16], and THz modulation of the Hubbard U in an organic Mott insulator [17–19].

In recent years, much attention has been drawn to 2D materials such as graphene, hexagonal boron nitride (h-BN), transition metal dichalcogenides (TMDs), silicene and phosphorene [20,21]. These 2D materials provide exciting opportunities from both electronic and optics perspectives [22–24]. Previous reports have suggested

* Corresponding author.

E-mail address: minjie.wang@stevens.edu (M. Wang).

that graphene and other 2D materials can realize all functions required for integrated photonic circuits (e.g., generation, modulation, and detection of photons), in various wavelength ranges including THz. These functions, combined with their unique electronic properties, such as gapless band structure and ultrahigh carrier mobilities, and other extraordinary mechanical, chemical and optical properties, may enable the newly functional 2D material-based electro-optic devices [25]. Particularly, 2D materials are also expected to provide exciting opportunities for diverse appealing prospects in THz applications [26]. For instance, CVD-grown monolayer MoS₂ and WSe₂ have been reported to have ultrafast transient THz conductivity, which is likely to be a key component of future high-frequency optoelectronic devices including photoreceivers, emitters, modulators as well as microwave and THz switches [27].

2. Graphene for THz applications

Graphene has attracted much attention since its first successful isolation from graphite in 2004 [28], and the following experimental investigation of its unique quantum electromagnetic properties [29,30] in 2005. Graphene is the first atomically thin material isolated and opened the door to the world of 2D materials. Carbon atoms in graphene are tightly sp²-bonded into hexagonal lattices, which can be regarded as two interleaving triangular lattices and provides graphene's stability. Graphene has the highest ratio of edge atoms of any allotrope, which leads to a hundred times more chemical reactivation than thicker sheets [31,32]. Graphene is a particularly interesting material for optics applications, since it possesses a broadband optical absorption property: graphene absorbs light at any frequency, including THz range. Besides, graphene is a zero-gap semiconductor with unique linear energy-momentum dispersion relation [25,33–35]. The existence of a Dirac point, where its conduction and valence bands meet, gives it a number of interesting properties such as tunable carrier densities [36–38] and predictable high nonlinearities compared to traditional semiconductors [39–41]. Also, graphene displays electron mobilities as high as 15,000 cm² V⁻¹ s⁻¹ at room temperature, with a theoretical potential limit of 200,000 cm² V⁻¹ s⁻¹, limited by acoustic photon scattering. These unique properties result in ultra-wideband accessibility provided by the e-h pair generation in graphene, which is gate controllable, at all wavelengths. Thus, graphene can have strong light interaction and special phenomenal such as light excitation of collective oscillations of carries, *i.e.*, plasmons in graphene [42,43]. Furthermore, it is possible to create an inversion of the conical electronic band around the Dirac point with optical excitation [33], leading to gain in THz range. These properties make graphene promising for novel applications in photonics and optoelectronics and attracted much attention. For instance, graphene ribbons were demonstrated to be potential broadband absorbers by canceling strong coupling at subwavelength scale [44], and graphene-based metamaterials are promising for developing new THz broadband polarization rotator [45]. In this section, we mainly discuss the recent progress of the graphene-based THz emitters, detectors, and modulators [46].

2.1. Graphene based THz-emitter

THz emitter is the core and starting point of the entire THz system. Researchers are devoting a lot of efforts to develop newer and better THz generation techniques in order to obtain THz waves of higher intensity and especially broader bandwidth. Generally speaking, three generations of THz emitters have been developed in the past: photoconductive antennas [47], nonlinear electro-optic crystal [48], and air plasma [49]. Nowadays, these sources are not efficient or strong enough to meet the demands of the

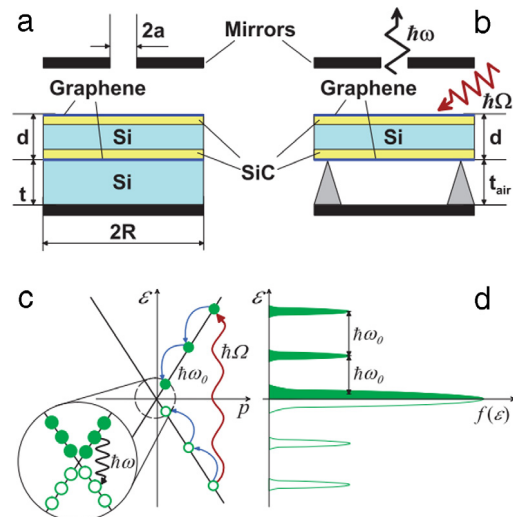


Fig. 1. Schematic view of the laser structures with Si separation layer (a) and with air separation layer (b), as well as the laser pumping scheme (c) and electron and hole distribution functions (d). Figures reprinted with permission from ref. [54] Copyright© 2009 The Japan Society of Applied Physics,

application. Hence, better THz emitters based on graphene and other 2D materials are expected, owing to their extraordinary electro-optical properties.

There have been several recent studies toward microscopic understanding of unique carrier dynamics in graphene for THz applications [50]. Early in 2007, optically or electrically pumped graphene was predicted to exhibit population inversion near the Dirac point owing to ultrafast carrier relaxation and relatively slow recombination lifetimes [51,52], which leads to a negativity of the real part of dynamic conductivity in a wide THz spectral range [53]. The dynamic conductivity comprises both interband and intraband contributions, and the negative real part of dynamic conductivity at sufficiently strong pumping implies that interband emission of photons with the energy $\hbar\omega$ overwhelms the intraband Drude absorption. That is, a positive gain is established in certain wavelength ranges. Based on these experimental and theoretical studies, an optically pumped THz laser based on an optically pumped graphene-heterostructure was proposed and substantiated with a Fabri-Perot resonant cavity design in 2009 [54]. A sketch of the structure is depicted in Fig. 1. Electrons and holes in graphene layers are first introduced by optical excitation with the energy of $\hbar\Omega$. After following optical phonon cascade, substantial electron and hole populations of the bottom conduction band and the top valence band, which can generate THz radiation, were obtained. The THz lasing is raised, if the ratio of the THz radiation power generated in the graphene layers to the THz power absorbed in the cavity and Si-layers is large enough.

Another design of THz lasers was proposed based on optically pumped multiple-graphene-layer structures with a metal slot-line waveguide or a dielectric waveguide [55]. Frequency dependences of the absorption in the waveguides and the gain-overlap factor were taken into account, demonstrating THz lasing at the low end of the THz frequency range at room temperatures. Moreover, the current-injection THz laser was also proposed to avoid drawbacks in optical pumping, such as complex setups that might be inconvenient and inefficient and high excessive energy that might produce marked heating [56,57], as an alternative of graphene channel transistor THz laser. A sketch of graphene-based p-i-n structures with electron and hole injection (double injection) is depicted in Fig. 2 [58]. The structure is based on a p-i-n junction produced by

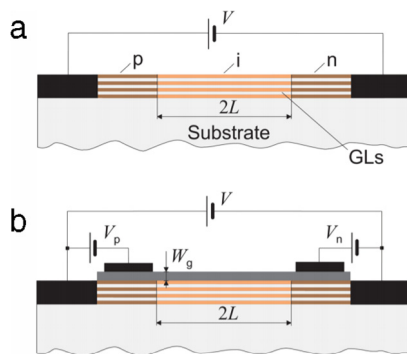


Fig. 2. Schematic view of the cross-sections of multiple graphene layers laser structures (a) with chemically doped n- and p-sections and (b) with such section electrically induced by the side gate-voltages. Figures reprinted with permission from ref. [58] Copyright© 2013 AIP Publishing LLC.

chemical doping or gating. Self-excitation of THz modes propagating in the substrate (in the direction perpendicular to the injection current) and lasing was demonstrated under certain conditions. Applied injection voltage between source and drain was in the order of only several mV to tens of mV.

Apart from these, Graphene plasmonic oscillators for THz generation were also proposed [51,59,60]. It was also shown that graphene possesses intrinsic plasmons that are tunable and adjustable [61]. Time-resolved picosecond photocurrents in freely suspended graphene contacted by stripline metal electrodes were observed, and electromagnetic radiation up to 1 THz was generated from an electron-hole plasma in the optically pumped graphene. The signal was AC-coupled to the metal striplines [62]. However, the interband absorption of graphene is limited to $e^2/4\hbar$, which corresponds to 2.3% absorption per layer for normal incident light [63–66], limiting its applications in THz lasers. We discuss it later in Section 2.4.

2.2. Graphene base THz-detector

In the past decades, many THz detectors have been developed based on a variety of principles ranging from bolometer THz detector, Schottky barrier THz detectors, pair braking THz detectors and Field-effect Transistor (FET) THz detectors. To characterize these THz detectors, two generalized performance parameters are commonly used: one is Noise Equivalent Power (NEP), which is related to the smallest power that can be detected, and the other is detectivity [67]. Other issues such as responding time, stability, cost and maintaining cost are also a concern. Despite the various appealing application of photodetection of THz radiation in communication, imaging, security, life sciences and medicine, the existing conventional THz and sub-THz detection systems have their own limits. For example, bolometric type of detectors is extremely sensitive to background radiation, temperature fluctuation, mechanical vibration and electrical interference, and the performance is even poorer at higher frequencies in the THz range [67]. Cooling to cryogenic temperatures becomes necessary in many situations. Schottky barrier THz detectors are hard to design, fabricate and operate. Utilization of FETs for THz spectroscopy seems much more promising compared to detectors described above, since they are very fast and highly responsive. In a series of pioneering papers [68–71], the prediction that plasma oscillations in a FET channel can produce the THz emission attracted a lot of interests. Several years later, both THz emission and detection in FETs were experimentally observed, at both cryogenic and room temperatures. It has been demonstrated that gate lengths can determine plasma frequency of the resonator. For gate lengths on the order of

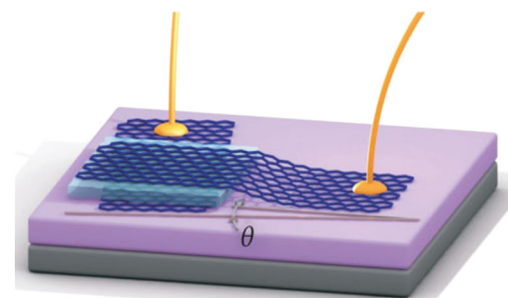


Fig. 3. Device schematics with an exaggerated angle θ between two graphene layers (separated by an h-BN tunnel barrier). Figures reprinted with permission from ref. [77] Copyright© 2014 Macmillan Publishers Limited.

1 or 0.1 μm , plasma oscillations were in THz region [72]. Based on these theoretical and experimental results, various structures for THz detection were proposed. Single-layer and bilayer graphene FET devices are commonly used for resonant THz detection, and simple top-gate antenna-coupled configuration is also utilized for broadband THz detection via excitation of over damped plasma waves [73–84]. To make these heterostructure devices, which can be actually regarded as a new type of THz detectors beyond normal FETs, e.g., high electron mobility transistor (HEMT), new types of 2D materials beyond graphene such as h-BN and their manipulating methods can be incorporated. For example, by carefully aligning the orientation of crystal lattices in two graphene layers separated by an h-BN layer, tunnel transistors that have resonant tunneling with both energy and momentum conservation can be constructed. This tunnel transistor does not have the fundamental limitation of a long carrier dwell time (picoseconds) in the quantum well, so it can potentially be scaled to operate for THz detection [77]. A sketch of tunnel transistor structure is depicted in Fig. 3. Similar heterostructures which comprise of a thin h-BN tunnel barrier sandwiched between two graphene layers (i.e., n-type and p-type doped) were investigated. Voltage tunable THz wave generation and detection were both reported [85]. Graphene channel transistors and graphene photodetectors were shown to operate in the THz range [86–91]. By further applying an external magnetic field, a graphene transistor can also be used as a frequency-tunable (0.76–33 THz) detector [92].

2.3. Graphene THz modulator

Besides the promising perspective of graphene THz lasers, another potentially important area of applications for graphene is THz modulation [93]. Generally, graphene optical modulators are classified by a modulation mechanism in which electrical elements are involved or not. For electro-optical graphene optical modulators, both interband transition and intraband transition have to be taken into account. Interband transition, which dominates the short wavelength absorption, is frequency-independent and can be calculated as $T \approx 1 - \pi\alpha \approx 0 : 977$ [63–66], where α is the fine-structure constant ($=e^2/4\hbar = 1/137 = 2.3\%$). For long wavelength cases, intraband transition is more important, and it can be described by the following equation for graphene in THz regime:

$$T(\omega) = \left(1 + \frac{\pi\alpha}{1 + n_{sub}} \frac{\sigma'(\omega)}{\frac{\pi e^2}{2h}}\right)^{-2} \quad (1)$$

where n_{sub} is the refractive index of the substrate. Drude model is commonly used for calculating graphene parameters in THz regime and it can be described by:

$$\tilde{\sigma}(\omega) = \frac{\sigma_0}{1 - i\omega\tau} \quad (2)$$

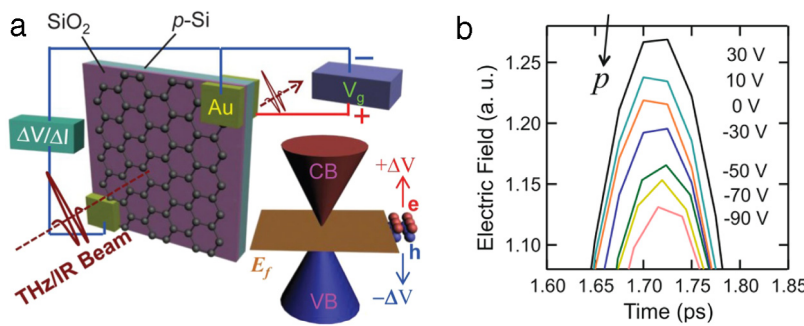


Fig. 4. (a) Sketch of the gated large-area graphene device fabricated, together with the incident and transmitted THz beams. (b) Gate-voltage-dependent THz wave transmission through single-layer graphene. Figures reprinted with permission from ref. [94] Copyright© 2012 Springer Business Media LLC.

where σ_0 is the DC conductivity and τ is the carrier scattering time. The charge carrier density in graphene can be easily modified by chemical or electronic gating [94,95], and the optical transition of graphene is mainly determined by doping level, as described by following equations:

$$\sigma_0 = en\mu = en \left(\frac{e\tau}{m^*} \right) \quad (3)$$

$$\mu = \frac{ev_f\tau}{\hbar\sqrt{\pi n}} \quad (4)$$

$$E_f = v_f\hbar\sqrt{\pi n} \quad (5)$$

where n is the carrier density, $v_f = 10^6$ m/s is the Fermi velocity for electrons in graphene, and μ is the carrier mobility. Graphene THz modulators based on intraband absorption have been proposed [94,96–98]. Various research groups have found different ways to modify the electronic properties of graphene by tuning the Fermi level and changing the charge type. Both electrically and chemically tunable Fermi level of graphene were used to modulate THz waveforms [94], and the modulation depth was very recently demonstrated to be enhanced by extraordinary transmission through ring apertures [99]. In a typical graphene/SiO₂/p-Si FET device configuration, transmitted THz electromagnetic waves can be modulated through a tunable gate voltage [94]. The sketch is depicted in Fig. 4(a). The THz wave is normal incident onto the device, and the transmitted wave is detected and recorded as a function of gate voltage (V_g), as shown in Fig. 4(b).

The modulation depth of the graphene/SiO₂/p-Si FET device is around 12% with the applied gate voltage around 110 V, and it has very recently been demonstrated to be enhanced by extraordinary transmission through ring apertures to more than 46% [99]. Graphene possesses intrinsic plasmons that are tunable and adjustable [61]. A combination of graphene with noble-metal nanostructures also supports surface plasmon modes that are also tunable by electronic gating in the THz regime [61,100]. It was also shown that the enhancement of attenuation and modulation depth in optically driven silicon modulators can be achieved by deposition of graphene on silicon, which gives another possibility of application graphene beyond modulating THz waves by itself [101]. A wide-band THz modulation in a frequency range from 0.2 to 2 THz and a maximum modulation depth of 99% were achieved by photodoping of graphene.

2.4. Enhancing THz-wave absorption

Graphene absorbs light at any frequency – from DC to sunlight. As introduced in the last section, the strength of absorption through the interband transition at any frequency is given by a combination of natural constants, $e^2/4\hbar$, which corresponds to 2.3% absorption per layer for normal incident light [63–66]. For intraband free-carrier absorption, the amount of absorption can

be ~30 times larger than interband absorption, depending on the carrier density [94]. While these numbers are impressively large, considering the atomically thin nature of graphene, they are too small for practical purposes, limiting its application in optoelectronic devices [95], such as photodetectors [102–104], optical antennas and solar cells. Therefore, enhancing light absorption in monolayer graphene has become one of the goals in this research field. For example, 100% light absorption can take place in a single patterned sheet of doped graphene nanodisks [105]. Surface plasmon enhanced absorption and suppressed transmission were predicted to take place in periodic arrays of graphene ribbons [106]. Monolayer graphene has been demonstrated to have total absorption in the near-infrared and visible wavelength ranges by critical coupling with a photonic-crystal guided resonance [107] and by doping/gating, graphene can exhibit higher absorption in the GHz-THz range [108–110]. Practical ways to obtain high optical absorption in graphene is required. Nearly 100% absorption of an electromagnetic wave in the THz frequency has been proposed for a system consisting of two monolayers of graphene [111]. Recently, it was also proposed that the absorption of graphene in the 0.01–0.1 THz range can be tuned from 0 to nearly 100% by varying the Fermi energy of graphene when the angle of incidence of the electromagnetic wave is kept within a total internal reflection geometry [112]. This is an economic and practical method, although sometimes a large mobility of graphene or a high Fermi energy is needed (E_f of 1 eV). Enhancement of THz-wave absorption up to 70% in monolayer graphene in 0.6–1.6 THz range has also been demonstrated by using a total reflection geometry with a parallelogram shaped TOPAS® substrate [86]. In this work, graphene transferred onto the surface of a parallelogram-shaped TOPAS® prism absorbs THz light significantly. Reflectance of graphene at 45° incident angle was measured using a two-prism TOPAS structure that can have 0 to 4 graphene reflections in the 0.6 to 1.6 THz range using a THz time-domain spectroscopy system. At each reflection, graphene absorbed ~71% of as-polarized THz beam uniformly in this frequency range and absorbed ~31% of a p-polarized THz beam at 45°. The amount of absorption per reflection was constant, as expected. Angular dependence of transmittance was also measured through a single-prism TOPAS® device with up to 2 graphene reflections. By rotating the single-prism TOPAS® device, the incident angle was varied from 25° to 70°. A dip of transmittance at around 50° was observed for s-polarized reflection. A sketch of the graphene-on-TOPAS® waveguide geometry is depicted in Fig. 5.

3. Other 2D materials for THz applications

In this section, we extend the review to other 2D materials beyond graphene. As we described above, h-BN is a wide band gap (5.9 eV) layered material [66] which is commonly used as

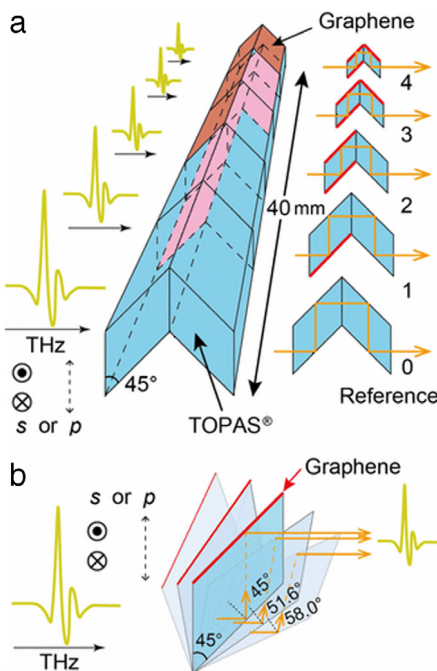


Fig. 5. Sketch of the graphene-on-TOPAS waveguide geometry. (a) Two pieces of TOPAS parallelograms are combined for four 45-degree reflections. One, two, three, or four pieces of graphene are put on the surfaces of TOPAS. Different numbers of graphene reflections can be selected by sliding the structure in a direction perpendicular to the incident THz beam. (b) One-parallelogram geometry for angular dependence measurements. The incidence angle to graphene is controlled by the rotatable stage under the waveguide. Figures reprinted with permission from ref. [86] Copyright© 2016 American Chemical Society.

insulating and protecting layer in heterostructures. It is comprised of constant boron (B) and nitrogen (N) atoms which build a hexagonal honey-comb structure [113,114]. Monolayer TMDs and black phosphorus are often direct bandgap semiconductors, which are particularly interesting for optoelectronic applications. 2D materials have similarities. For examples, similar to graphene, many TMDs can be synthesized by both top-down methods (typically, exfoliation) and bottom-up methods (typically, CVD growth) [115–119], owing to the surface energy similar to that of graphene ($65\text{--}120 \text{ mJ/m}^2$) [120–123]. However, there are differences in many properties between graphene and other 2D materials. For instance, optical absorption in monolayer semiconducting TMDs is much stronger than graphene. Due to band gap resonances, it can reach over 10% compared to that of graphene (2.3%). Moreover, electron mobility in TMDs is relatively low ($0.1\text{--}100 \text{ cm}^2/\text{Vs}$) at room temperature compared to graphene. Previous demonstrations suggest that other materials can have similar THz applications as graphene, and they can provide properties and functions complementary to that of graphene based ones.

As a typical TMD, molybdenum disulfide (MoS_2) is heavily investigated for its properties and potential in THz application [124]. By using an ultrafast two-dimensional visible/far-IR spectroscopy, relaxation dynamics of the photo-excited carriers in MoS_2 was measured and electron/phonon coupling was directly observed, giving us comprehensions to THz photon dynamics in MoS_2 [125]. Exciton-exciton annihilation was identified experimentally in ultrafast transient absorption measurements [126]. The decay time is on the scale of several tens of ps, which corresponds to the frequency range in sub-THz. In the same year, ultrafast charge carrier dynamics in monolayers and trilayers of MoS_2 and WSe_2 was measured to be $<1 \text{ ps}$ by Docherty et al. using a combination of time-resolved photoluminescence and THz spectroscopy [27], and

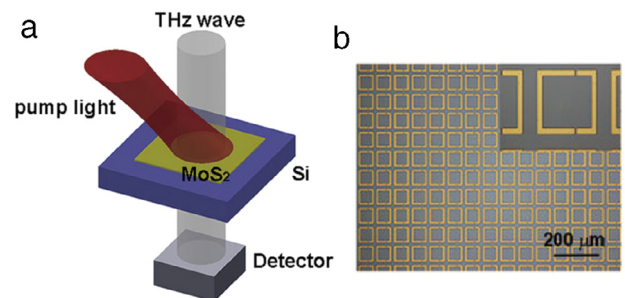


Fig. 6. (a) Schematic of Optically tuned terahertz modulator based on annealed multilayer MoS_2 /metal hybrid metamaterial structure. (b) Optical image of a section of the metamaterial and detail of a unit cell. Figures reprinted with permission from ref. [127] Copyright© 2016 Nature Publishing Group.

this time scale corresponds to a higher frequency range ($>1 \text{ THz}$). Two years later, optically tuned THz modulator based on large-area multilayer CVD-grown MoS_2 on silicon substrate was experimentally demonstrated [127]. It was demonstrated that THz transmission could be modulated up to 87% by changing the power of the pumping laser up to 4.56 W and modulation depth can be triply enhanced by annealing treatment of MoS_2 as a p-doping method compared with the bare silicon. Another publication about optically pumped Si- MoS_2 THz modulator obtained a high modulation depth ($\sim 75\%$) under a low pumping power of 0.24 W cm^{-2} [128]. MoS_2 was chosen as an example 2D material here to analyze this hybrid tunable THz structure, but the discussion can be extended to any other 2D-materials. Modulation depth levels larger than 2X the intrinsic modulation depth by the MoS_2 film and low insertion loss ($<3 \text{ dB}$) can be realized by utilizing this structure [26]. A typical sketch and optical image of fabricated MoS_2 /metal hybrid structures are shown in Fig. 6.

THz detection using 2D materials are also widely investigated. For instance, an antenna-coupled mechanical resonators based on 2D materials was proposed by Hassel et al. recently [129]. Both coherent and incoherent detection regimes were analyzed, but the operation speed was expected to be much lower than that in graphene based devices. Devices on flexible substrates were also fabricated and optimized, giving people more control over technology and application [130].

4. Conclusions and future prospects

In this review, we have discussed applications in THz technology of various kinds of 2D materials. It is both theoretically and experimentally demonstrated that graphene and other 2D materials can be utilized for THz emitting, detecting and modulating by kinds of meanings, and newer and better devices can be expected since there are many groups in the world working in this area now. Nonetheless, there is still a significant need for mechanism and technology improvement in order to obtain well-developed industrially applicable devices. For example, modulation speed and energy consumption of these devices are not that ideal compared to existing commercial ones. Several challenges remain on the road to industrial application. One of the critically important issues is the stability and quality of 2D materials. Although tones of efforts have been devoted to synthesizing single-crystal, large-size 2D materials, it is still hard to obtain single-crystal graphene larger than millimeter size, and the grain size and sample size of h-BN and TMDs are even smaller. CVD grown samples can have relatively large sizes, but they have their own drawbacks. Defects and contaminations which can cause sample degradation with time are still inevitable, making it difficult to have stable devices. Thus, there is still a long way to go before we can have matured 2D material THz devices.

References

- [1] M. Tonouchi, Nat. Photonics 1 (2007) 97.
- [2] B. Ferguson, X.C. Zhang, Nat. Mater. 1 (2002) 26.
- [3] D. Mittleman, Sensing with Terahertz Radiation, Springer, Berlin, 2003.
- [4] K. Sakai, Terahertz Optoelectronics, Springer, Berlin, 2005.
- [5] C.A. Schmuttenmaer, Chem. Rev. 104 (2004) 1759.
- [6] P.H. Siegel, IEEE Trans. Microw. Theory 50 (2002) 910.
- [7] P.H. Siegel, IEEE Trans. Microw. Theory 52 (2004) 2438.
- [8] S.K. Ray, T.N. Adam, R.T. Troeger, J. Kolodzey, G. Looney, A. Rosen, J. Appl. Phys. 95 (2004) 5301.
- [9] S.D. Brorson, J.C. Zhang, S.R. Keiding, Appl. Phys. Lett. 64 (1994) 2385.
- [10] Y.T. Li, J.W. Shi, C.Y. Huang, N.W. Chen, S.H. Chen, J.I. Chyi, Y.C. Wang, C.S. Yang, C.L. Pan, IEEE J. Quantum Electron. 46 (2010) 19.
- [11] N. Kishimoto, S. Suzuki, A. Teranishi, M. Asada, Appl. Phys. Express 1 (2008).
- [12] J. Nishizawa, P. Plotka, T. Kurabayashi, IEEE Trans. Electron Devices 49 (2002) 1102.
- [13] X. Oriols, A. Alarcon, L. Baella, Solid-State Electron. 51 (2007) 1287.
- [14] L. Berge, S. Skupin, C. Kohler, I. Babushkin, J. Herrmann, Phys. Rev. Lett. (2013) 110.
- [15] X.H. Yao, M. Tokman, A. Belyanin, Phys. Rev. Lett. (2014) 112.
- [16] M.N. Gadalla, M. Abdel-Rahman, A. Shamim, Sci. Rep. UK 4 (2014).
- [17] P. Kuzel, F. Kadlec, Cr. Phys. 9 (2008) 197.
- [18] M. Rahm, J.S. Li, W.J. Padilla, J. Infrared Millim. Te. 34 (2013) 1.
- [19] R. Singla, et al., Phys. Rev. Lett. (2015) 115.
- [20] A. Gupta, T. Sakthivel, S. Seal, Prog. Mater. Sci. 73 (2015) 44.
- [21] R. Mas-Balleste, C. Gomez-Navarro, J. Gomez-Herrero, F. Zamora, Nanoscale 3 (2011) 20.
- [22] S.J. Kim, K. Choi, B. Lee, Y. Kim, B.H. Hong, Annu. Rev. Mater. Res. 45 (2015) 63.
- [23] W.G. Kim, S. Nair, Chem. Eng. Sci. 104 (2013) 908.
- [24] M. Chhowalla, D. Jena, H. Zhang, Nat. Rev. Mater. 1 (2016) 16052.
- [25] A.C. Ferrari, et al., Nanoscale 7 (2015) 4598.
- [26] S. Arezoomandan, P. Gopalan, K. Tian, A. Chanana, A. Nahata, A. Tiwari, B. Sensale-Rodriguez, IEEE J. Sel. Top. Quantum Electron. (2017) 23.
- [27] P.P. Callum, J. Docherty, Hannah J. Joyce, Ming-Hui Chiu, Chang-Hsiao Chen, Ming-Yang Lee, Lain-Jong Li, Laura M. Herz, Michael B. Johnston, ACS Nano 8 (2014) 11147.
- [28] K.S. Novoselov, A.K. Geim, S.V. Morozov, D. Jiang, Y. Zhang, S.V. Dubonos, I.V. Grigorieva, A.A. Firsov, Science 306 (2004) 666.
- [29] K.S. Novoselov, A.K. Geim, S.V. Morozov, D. Jiang, M.I. Katsnelson, I.V. Grigorieva, S.V. Dubonos, A.A. Firsov, Nature 438 (2005) 197.
- [30] Y.B. Zhang, Y.W. Tan, H.L. Stormer, P. Kim, Nature 438 (2005) 201.
- [31] L. Zhang, L.J. Long, W.Y. Zhang, D. Du, Y.H. Lin, Electroanal 24 (2012) 1745.
- [32] O. Akhavan, E. Ghaderi, A. Esfandiar, J. Phys. Chem. B 115 (2011) 6279.
- [33] Z.P. Sun, A. Martinez, F. Wang, Nat. Photonics 10 (2016) 227.
- [34] F.N. Xia, H. Wang, D. Xiao, M. Dubey, A. Ramasubramaniam, Nat. Photonics 8 (2014) 899.
- [35] F. Bonaccorso, Z. Sun, T. Hasan, A.C. Ferrari, Nat. Photonics 4 (2010) 611.
- [36] L. Wang, Z. Sofer, P. Simek, I. Tomandl, M. Pumera, J. Phys. Chem. C 117 (2013) 23251.
- [37] S.L. Lei, B. Li, E.J. Kan, J. Huang, Q.X. Li, J.L. Yang, J. Appl. Phys. (2013) 113.
- [38] C. Baeumer, S.P. Rogers, R.J. Xu, L.W. Martin, M. Shim, Nano Lett. 13 (2013) 1693.
- [39] K.J.A. Ooi, L.K. Ang, D.T.H. Tan, Appl. Phys. Lett. (2014) 105.
- [40] W.J. Kim, Y.M. Chang, J. Lee, D. Kang, J.H. Lee, Y.W. Song, Nanotechnology 2 (2012) 3.
- [41] S.F. Wu, L. Mao, A.M. Jones, W. Yao, C.W. Zhang, X.D. Xu, Nano Lett. 12 (2012) 2032.
- [42] S.M. Rao, J.J.F. Heitz, T. Roger, N. Westerberg, D. Faccio, Opt. Lett. 39 (2014) 5345.
- [43] F.N.A. Xia, IEEE Photon. Conf. (2013) 543.
- [44] X. Shi, L. Ge, X. Wen, D. Han, Y. Yang, Opt. Express 24 (2016) 26357.
- [45] X. Wen, J. Zheng, Opt. Express 22 (2014) 28292.
- [46] M. Hasan, S. Arezoomandan, H. Condori, B. Sensale-Rodriguez, Nano Commun. Netw. 10 (2016) 68.
- [47] P.R. Smith, D.H. Auston, M.C. Nuss, IEEE J. Quantum Electron. 24 (1988) 255.
- [48] A. Rice, Y. Jin, X.F. Ma, X.C. Zhang, D. Bliss, J. Larkin, M. Alexander, Appl. Phys. Lett. 64 (1994) 1324.
- [49] N. Karpowicz, et al., Appl. Phys. Lett. (2008) 92.
- [50] T. Otsuji, S.A.B. Tombet, A. Satou, H. Fukidome, M. Suemitsu, E. Sano, V. Popov, M. Ryzhii, V. Ryzhii, J. Phys. D: Appl. Phys. (2012) 45.
- [51] V. Ryzhii, M. Ryzhii, T. Otsuji, J. Appl. Phys. (2007) 101.
- [52] M. Ryzhii, V. Ryzhii, Jpn. J. Appl. Phys. 2 46 (2007) L151.
- [53] A. Satou, F.T. Vasko, V. Ryzhii, Phys. Rev. B (2008) 78.
- [54] A.A. Dubinov, V.Y. Aleshkin, M. Ryzhii, T. Otsuji, V. Ryzhii, Appl. Phys. Express 2 (2009).
- [55] V. Ryzhii, A.A. Dubinov, T. Otsuji, V. Mitin, M.S. Shur, J. Appl. Phys. 107 (2010).
- [56] T. Otsuji, S.B. Tombet, A. Satou, V. Ryzhii, M. Ryzhii, P. IEEE Les. Eastm. (2012).
- [57] V. Ryzhii, M. Ryzhii, V. Mitin, T. Otsuji, J. Appl. Phys. 110 (2011).
- [58] V. Ryzhii, I. Semenikhin, M. Ryzhii, D. Svitsov, V. Vyurkov, A. Satou, T. Otsuji, J. Appl. Phys. 113 (2013).
- [59] F. Rana, IEEE Trans. Nanotechnol. 7 (2008) 91.
- [60] V. Ryzhii, A. Satou, W. Knap, M.S. Shur, J. Appl. Phys. 99 (2006).
- [61] A.N. Grigorenko, M. Polini, K.S. Novoselov, Nat. Photonics 6 (2012) 749.
- [62] L. Prechtel, L. Song, D. Schuh, P. Ajayan, W. Wegscheider, A.W. Holleitner, Nature Commun. 3 (2012).
- [63] H. Choi, F. Borondics, D.A. Siegel, S.Y. Zhou, M.C. Martin, A. Lanzara, R.A. Kaindl, Appl. Phys. Lett. 94 (2009).
- [64] Z.Q. Li, E.A. Henriksen, Z. Jiang, Z. Hao, M.C. Martin, P. Kim, H.L. Stormer, D.N. Basov, Nat. Phys. 4 (2008) 532.
- [65] K.F. Mak, M.Y. Sfeir, Y. Wu, C.H. Lui, J.A. Misewich, T.F. Heinz, Phys. Rev. Lett. 101 (2008).
- [66] R.R. Nair, P. Blake, A.N. Grigorenko, K.S. Novoselov, T.J. Booth, T. Stauber, N.M.R. Peres, A.K. Geim, Science 320 (2008) 1308.
- [67] M.G. Krishna, S.D. Kshirsagar, S.P. Tewari, in: S. Gateva (Ed.), Photodetectors, 2012.
- [68] M. Dyakonov, M. Shur, Phys. Rev. Lett. 71 (1993) 2465.
- [69] M.I. Dyakonov, M.S. Shur, Phys. Rev. B 51 (1995) 14341.
- [70] M. Dyakonov, M. Shur, IEEE Trans. Electron Devices 43 (1996) 380.
- [71] M.I. Dyakonov, M.S. Shur, IEEE Trans. Electron Devices 43 (1996) 1640.
- [72] M.I. Dyakonov, Semiconductors+ 42 (2008) 984.
- [73] R.M. Feenstra, D. Jena, G. Gu, J. Appl. Phys. (2012) 111.
- [74] V. Ryzhii, T. Otsuji, M. Ryzhii, M.S. Shur, J. Phys. D: Appl. Phys. (2012) 45.
- [75] V. Ryzhii, A. Satou, T. Otsuji, M. Ryzhii, V. Mitin, M.S. Shur, J. Phys. D: Appl. Phys. (2013) 46.
- [76] L. Britnell, R.V. Gorbachev, A.K. Geim, L.A. Ponomarenko, A. Mishchenko, M.T. Greenaway, T.M. Fromhold, K.S. Novoselov, L. Eaves, Nature Commun. 4 (2013).
- [77] A. Mishchenko, et al., Nat. Nanotechnol. 9 (2014) 808.
- [78] B. Fallahazad, et al., Nano Lett. 15 (2015) 428.
- [79] V. Ryzhii, T. Otsuji, V.Y. Aleshkin, A.A. Dubinov, M. Ryzhii, V. Mitin, M.S. Shur, Appl. Phys. Lett. 104 (2014).
- [80] V. Ryzhii, T. Otsuji, M. Ryzhii, V. Mitin, M.S. Shur, J. Appl. Phys. 118 (2015).
- [81] A. Tomadin, A. Tredicucci, V. Pellegrini, M.S. Vitiello, M. Polini, Appl. Phys. Lett. 103 (2013).
- [82] V. Ryzhii, T. Otsuji, M. Ryzhii, V.Y. Aleshkin, A.A. Dubinov, D. Svitsov, V. Mitin, M.S. Shur, 2D Mater. 2 (2015).
- [83] B. Sensale-Rodriguez, Appl. Phys. Lett. 103 (2013).
- [84] L. Vicarelli, M.S. Vitiello, D. Coquillat, A. Lombardo, A.C. Ferrari, W. Knap, M. Polini, V. Pellegrini, A. Tredicucci, Nat. Mater. 11 (2012) 865.
- [85] D. Yadav, S.B. Tombet, T. Watanabe, S. Arnold, V. Ryzhii, T. Otsuji, 2D Mater. 3 (2016).
- [86] Y. Harada, et al., ACS Photonics 4 (2017) 121.
- [87] F. Schwierz, Nat. Nanotechnol. 5 (2010) 487.
- [88] Y.Q. Wu, Y.M. Lin, A.A. Bol, K.A. Jenkins, F.N. Xia, D.B. Farmer, Y. Zhu, P. Avouris, Nature 472 (2011) 74.
- [89] Y.Q. Wu, et al., Nano Lett. 12 (2012) 3062.
- [90] V. Ryzhii, T. Otsuji, N. Ryabova, M. Ryzhii, V. Mitin, V. Karasik, Infrared Phys. Technol. 59 (2013) 137.
- [91] V. Ryzhii, N. Ryabova, M. Ryzhii, N.V. Baryshnikov, V.E. Karasik, V. Mitin, T. Otsuji, Opto-Electron Rev. 20 (2012) 15.
- [92] Y. Kawano, Nanotechnology (2013) 24.
- [93] M. Liu, X.B. Yin, E. Ulin-Avila, B.S. Geng, T. Zentgraf, L. Ju, F. Wang, X. Zhang, Nature 474 (2011) 64.
- [94] L. Ren, Q. Zhang, S. Nanot, I. Kawayama, M. Tonouchi, J. Kono, J. Infrared Millim. Te. 33 (2012) 846.
- [95] R.R. Hartmann, J. Kono, M.E. Portnoi, Nanotechnology 25 (2014).
- [96] V. Ryzhii, M. Ryzhii, A. Satou, T. Otsuji, A.A. Dubinov, V.Y. Aleshkin, J. Appl. Phys. 106 (2009).
- [97] V. Ryzhii, M. Ryzhii, A. Satou, T. Otsuji, N. Kirova, J. Appl. Phys. 105 (2009).
- [98] B. Sensale-Rodriguez, T. Fang, R.S. Yan, M.M. Kelly, D. Jena, L. Liu, H.L. Xing, Appl. Phys. Lett. 99 (2011).
- [99] W.L. Gao, et al., Nano Lett. 14 (2014).
- [100] W.L. Gao, et al., Nano Lett. 14 (2014) 1242.
- [101] P. Weis, J.L. Garcia-Pomar, M. Hoh, B. Reinhard, A. Brodyanski, M. Rahm, ACS Nano 6 (2012) 9118.
- [102] G. Pirruccio, L.M. Moreno, G. Lozano, J.G. Rivas, ACS Nano 7 (2013) 4810.
- [103] T. Mueller, F.N.A. Xia, P. Avouris, Nat. Photonics 4 (2010) 297.
- [104] F.N. Xia, T. Mueller, Y.M. Lin, A. Valdes-Garcia, P. Avouris, Nat. Nanotechnol. 4 (2009) 839.
- [105] S. Thongrattanasiri, F.H.L. Koppens, F.J.G. de Abajo, Phys. Rev. Lett. 108 (2012).
- [106] A.Y. Nikitin, F. Guinea, F.J. Garcia-Vidal, L. Martin-Moreno, Phys. Rev. B 85 (2012).
- [107] J.R. Piper, S.H. Fan, ACS Photonics 1 (2014) 347.
- [108] U. Ralevic, G. Isic, B. Basic, D. Gvozdic, R. Gajic, J. Phys. D: Appl. Phys. 48 (2015).
- [109] J. Gosciniak, D.T.H. Tan, B. Corbett, J. Phys. D: Appl. Phys. 48 (2015).
- [110] S.Y. Luo, Y.N. Wang, X. Tong, Z.M. Wang, Nanoscale Res. Lett. 10 (2015) 1.
- [111] C.B. Reynolds, M.S. Ukhtary, R. Saito, J. Phys. D: Appl. Phys. 49 (2016).

- [112] M.S. Ukhtary, E.H. Hasdeo, A.R.T. Nugraha, R. Saito, *Appl. Phys. Express* 8 (2015).
- [113] A. Zobelli, A. Gloter, C.P. Ewels, G. Seifert, C. Colliex, *Phys. Rev. B* 75 (2007).
- [114] A.V. Krasheninnikov, F. Banhart, *Nat. Mater.* 6 (2007) 723.
- [115] V.K. Kumar, S. Dhar, T.H. Choudhury, S.A. Shivashankar, S. Raghavan, *Nanoscale* 7 (2015) 7802.
- [116] J. Krustok, et al., *Appl. Phys. Lett.* 109 (2016).
- [117] P.S. Liu, et al., *Int. Electron. Devices Meet.* (2014).
- [118] S. Tongay, et al., *Nano Lett.* 14 (2014) 3185.
- [119] W.H. Yang, et al., *Nano Lett.* 16 (2016) 1560.
- [120] Y. Hernandez, et al., *Nat. Nanotechnol.* 3 (2008) 563.
- [121] J.N. Coleman, et al., *Science* 331 (2011) 568.
- [122] G. Cunningham, M. Lotya, C.S. Cucinotta, S. Sanvito, S.D. Bergin, R. Menzel, M.S.P. Shaffer, J.N. Coleman, *ACS Nano* 6 (2012) 3468.
- [123] E. Diaz, S. Ordóñez, A. Vega, *J. Colloid Interface Sci.* 305 (2007) 7.
- [124] P.N.J.H. Strait, F. Rana, *Phys. Rev. B* 90 (2014).
- [125] X. Guo, H. Chena, X. Wen, J. Zheng, *J. Chem. Phys.* 142 (2015) 212447.
- [126] D. Sun, Y. Rao, Georg A. Reider, Gugang Chen, Y. You, L. Brezin, A.R. Harutyunyan, T.F. Heinz, *Nano Lett.* 14 (2014) 5625.
- [127] Y. Cao, S. Gan, Z. Geng, J. Liu, Y. Yang, Q. Bao, H. Chen, *Sci. Rep. UK* 6 (2016) 22899.
- [128] S. Chen, F. Fan, Y. Miao, X. He, K. Zhang, S. Chang, *Nanoscale Res. Lett.* (2016) 4713.
- [129] M.O. Juha Hassel, Teemu Elo, Heikki Seppä, Pertti J. Hakonen, *AIP Adv.* 7 (2017).
- [130] G. Deligeorgis, A. Stavrakaki, F. Iacovella, In *Advanced Materials and Processes for RF and THz Applications*, IMWS-AMP, IEEE, Suzhou, China, 2015.